

Article

The Effect of Pressurized Decarbonization of CO on Inhibiting the Adhesion of Fine Iron Ore Particles

Qiyang Xu, Zhiping Li, Zhuangzhuang Liu, Jianjun Wang and Haichuan Wang *

School of Metallurgical Engineering, Anhui University of Technology, Ma'anshan 243002, China; qiyang.xu@163.com (Q.X.); 15065785743@163.com (Z.L.); LiuZhuangzhuangNEU@163.com (Z.L.); Wangjj@ahut.edu.cn (J.W.)

* Correspondence: which@ahut.edu.cn; Tel.: +86-0555-2117-288

Received: 11 June 2018; Accepted: 5 July 2018; Published: 6 July 2018



Abstract: In this research, Australian fine iron ore is reduced by pressured carbon monoxide in a fluidized bed. This research aims to obtain the influence law of gas linear velocity, reduction pressure, reduction temperature, particle size, and reduction time on the reduction effect and the economic, convenient, and effective operating parameters, as well as clarify the effect of the pressurized decarbonization of CO, which inhibits the adhesion of fine iron ore particles during the reduction process. The experimental results show that the preferable operating parameters are a linear velocity of 0.8 m/s, reduction pressure of 0.2 MPa, reduction temperature of 1023 K, and particle size of 0.18 mm–0.66 mm. The graphite produced by the carbon precipitation reaction of carbon monoxide hinders the diffusion of iron atoms and avoids the direct contact between the iron atoms, thereby effectively controlling the sticking.

Keywords: carbon monoxide; linear velocity; reduction pressure; reduction temperature; inhibition mechanism

1. Introduction

The fluidized direct reduction process plays an important metallurgical role in the magnetization roasting of fine iron ore, the preheating of iron ore, the low-grade prerreduction, and the production of direct reduced iron [1–4]. One million and five hundred thousand tons of FINEX production line (a non-blast furnace ironmaking process) was built and put into commercial production in Pohang, South Korea, in April 2007. Compared with blast furnace ironmaking process, FINEX ironmaking [5] can save raw fuel costs, broaden the use of raw materials and fuels, and save sintering and coking processes, which emit the most emissions. It can significantly reduce pollutant emissions and realize clean production, representing a feasible innovative green ironmaking technology with low environmental emissions. However, in the process of the high-temperature fluidized reduction of iron ore powder, sticking loss may occur more easily, reducing the reduction efficiency and hindering the continuous operation of the process [6–10]. This has become the most important obstacle for the industrialized application of fluidized iron smelting technology. In order to effectively inhibit the sticking loss, many scholars have conducted research at atmospheric pressure [11–13]. However, in the process of non-blast furnace ironmaking, the gas-based reduction process is operated with pressure. Moreover, many experts have mostly studied the mechanism of inhibiting sticking loss based on atmospheric pressure, which is not in accordance with the actual production. Therefore, it is of great significance to study the mechanism of pressure change in inhibiting sticking among fine iron ore particles.

Due to the high cost and difficult operation of the experimental equipment under high pressure at the early stage, the test methods could not meet the high-pressure conditions. There are

few reports on the flowing characteristics of the pressure fluidized bed. In the 1980s, with the application of pressurized fluidized bed combustion and the development of pressurized gasification technology [14,15], many scholars carried out research on the characteristics of gas-solid flow under the conditions of pressure operation, including the minimum fluidization velocity, expansion height, and microtopography. The work of Sidorenko and other studies have shown that the minimum fluidization velocity of particle B decreases with increasing pressure when the operating pressure is between 101 kPa and 2100 kPa, while the pressure has no effect on particle A [16]. By observing the diameter and velocity of the bubbles in the bed of type B particles, Kawabata and others [17] demonstrated that the expansion height increases with increasing pressure. Studies by Krebs, Lee, and Gong Ming [18–20] showed that the optical structure of pitch carbon is an isotropic region and a mesophase globule at low carbonization pressure. With the increase of the carbonization pressure, the percentage of mesophase globules increases, and the coarse-grained mosaic structures increase slowly. The microstructure of pitch carbon changes from an anisotropic streamlined to a coarse-grained mosaic structure. Moreover, under low pressure, pitch carbon mainly exists in a streamlined structure, and the high-pressure coarse-grained mosaic structure coexists with a fine mosaic structure. These studies are mainly used in petroleum, chemical, coal, and other fields. They show their advantages in process intensification, production capacity improvement, product quantity, and economic benefits. However, in the process of the fluidized reduction of fine iron ore, the study of the mechanism of pressure change in inhibiting sticking among fine iron ore particles has rarely been reported.

For energy saving and environmental protection, as well as simple and efficient production, carbon monoxide is used as a reducing gas and varying gas velocities, reduction pressures, reduction temperatures, and particle sizes of fine iron ore articles are selected in the experiment. Through the investigation of the metallization rate, sticking ratio, and morphology in the hot state visual pressurized fluidized bed experiment device of self-design, the optimum direction of operation parameters is studied, and the economic, convenient, and effective operation parameters are obtained. And under different pressure conditions, the mechanism of carbon monoxide reduction in inhibiting sticking among fine iron ore particles and the mechanism of pressurized carbon monoxide in inhibiting sticking loss are further analyzed, providing data and a theoretical basis for the industrialization of the direct reduction process.

2. Experiment

2.1. Experimental Materials

The reduction fine iron ore powder used was OMC fine iron ore (a kind of Australian fine iron ore powder). Its chemical composition and SEM graph are shown in Table 1 and Figure 1, respectively. The selected OMC fine iron ore particle sizes are 0.12–0.15 mm, 0.15–0.18 mm, 0.18–0.66 mm, and 0.66–1.00 mm, the reducing gas is pure carbon monoxide, and the protective gas is nitrogen with a purity of 99.99%.

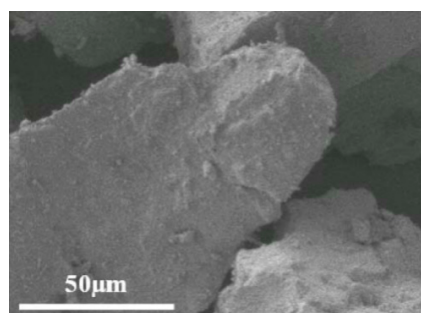


Figure 1. SEM graph of the OMC fine iron ore before reduction.

Table 1. Chemical composition of the Australian fine iron ore powder (mass %).

Compositions	TFe	FeO	SiO ₂	CaO	Al ₂ O ₃	MgO	MnO	P	S
Mass %	57.59	0.15	4.70	0.035	2.61	0.05	1.055	0.076	0.031

2.2. Experimental Device

The main device of the study is a pressurized visible fluidized bed with a double stainless steel pipe employed as the reactor. The inner pipe is a fluidized bed. The gas is preheated through the inter layer between the outer tube and the inner tube and flows into the fluidized bed. The outer tube contains heated cabinets. The different flows of carbon monoxide and nitrogen are regulated using multiple sets of flow meters to ensure that the composition content and velocity meet the experimental requirements. The inlet flow rate of the fluidized bed is controlled with the gas mass flow controller through the inner tube reduction of iron ores. The reduction temperature in the fluidized bed is measured with a thermocouple. The preheating and cooling of fine iron ores in the fluidized bed are conducted by passing through high-purity nitrogen for exhaust and protection. The observation window is used to evaluate the fluidized reduction sticking situation. The schematic of the pressurized fluidized reduction experiment and the device are shown in Figure 2.

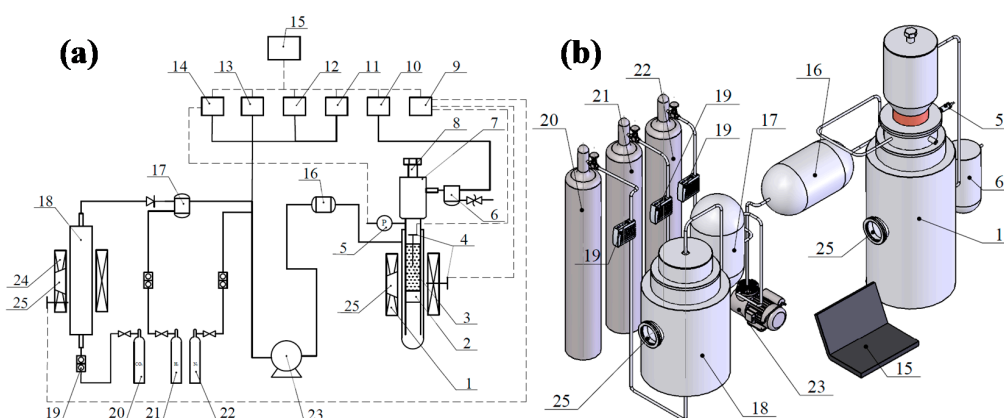


Figure 2. Experimental setup: (a) flow chart; (b) fluidized bed reactor. 1. Gas mixing and preheating chamber; 2. gas mixing hole; 3. fluidized bed; 4. K-type thermal couple; 5. pressure sensor; 6. gravity filter; 7. feeding and sampling port; 8. pressure seal cap; 9. temperature change recorder; 10. gas analyzer; 11. H₂ gas analysis recorder; 12. CO₂ gas analysis recorder; 13. CO gas analysis recorder; 14. pressure change analysis recorder; 15. computer; 16. gas dryer; 17. gasholder; 18. CO generated furnace; 19. gas mass flowmeter; 20. CO₂ gas cylinders; 21. H₂ gas cylinders; 22. N₂ gas cylinders; 23. booster pump; 24. carbon monoxide furnace; 25. observation window.

2.3. Experimental Programs and Methods

About 25 g fine iron ore powder was taken in each experiment. Before the test, the fluidized bed was heated to the setting temperature, and nitrogen was input under pressure for leakage detection. When the leakage detection was finished, the powder was added and the gas is input for the reduction. At the end of the test, the samples after the reduction were analyzed by ferric chloride titration and the potassium dichromate volumetric method, which led to metallic iron (M_{Fe}) and total iron (T_{Fe}), and then the metallization rate (η) ($\eta = M_{Fe}/T_{Fe}$) was calculated. The sticking ratio was calculated using the following formula:

$$\Omega = M_{sticking}/M_{total} \quad (1)$$

where Ω is the sticking ratio, $M_{sticking}$ is the quantity of sticking material after reduction, which can be used to measure the sticking material mass of the fine iron ore after reduction, and M_{total} is the total

quantity of material after reduction, which can be used to measure the total material mass of the fine iron ore after reduction.

The total quantity of material after reduction was calculated as follows:

$$M_{total} = M_{sticking} + M_{unstickng} \quad (2)$$

where $M_{unstickng}$ is the quantity of unsticking material after reduction, which can be used to measure the unsticking material mass of the fine iron ore after reduction.

In order to reduce the experimental error, repeated measurements were performed three times. The pressure in the experiments is not expressed in absolute values, and the atmosphere is set as 0 MPa.

After the raw materials were cooled by nitrogen protection, the inner tube of the double-layer fluidized bed is opened and the weight of the unsticking material particles and sticking material particles were obtained. Finally, the sticking ratio was calculated. The smaller the sticking ratio, the better the fluidization effect. Therefore, the metallization rate and bond ratio were selected as the indexes to judge the effect of the fluidization reduction. The optimum operation parameters of the fluidized reduction of energy-bearing waste plastics were optimized. Under the optimum operation parameters, the sticking mechanism of the fine iron ore was analyzed. The inhibition effect of the carbon evolution reaction was tested by means of microscopic analysis combined with a characterization experiment to determine the chemical characteristics of the gas-solid reaction. The surface microstructure of the particles was observed and analyzed by environmental scanning electron microscopy (ESEM) (FEI, Quanta 250), and the microstructure of the particles was observed and analyzed by a light microscope (LM) (CarlZeiss, Axio, Imager, A1). The phase composition of particles was analyzed by means of an X-ray diffraction analyzer (X, Pert, Pro, MPDalytical, Cu, 2 theta: 10°–90°), and the mechanism of carbon precipitation inhibiting the sticking loss was expounded.

3. Experimental Results

3.1. Influence of the Gas Linear Velocity

The first step was to set the temperature to 1023 K; when the temperature reached the setting value, the powder was added, the observation window was tightened, and the nitrogen was introduced. The proper range of gas linear velocity was determined by adjusting the gas flowing rate to observe the flowing state of the fine iron ore particles. The experiment showed that the linear velocity is lower than 0.5 m/s when the particle size is between 0.66 mm and 1.00 mm, and no fluidization appears. When the particle size is 0.12 mm–0.15 mm, the linear velocity is larger than 1.5 m/s, and there is the presence of fine iron ore in the observation window, which indicates that when the gas velocity is larger than 1.5 m/s, the fine iron ore particles will be blown out from the fluidized bed before the particles are reduced. Therefore, the linear velocity of the reducing gas was selected to be 0.5 m/s–1.5 m/s.

Pure carbon monoxide was used to reduce the OMC fine iron ore with a reduction pressure of 0 MPa, particle size of 0.18 mm–0.66 mm, and reduction temperature of 1023 K. The experimental results are shown in Figure 3. It can be seen from Figure 3 that as the linear velocity increases, the metallization rate first increases and then decreases, and the sticking ratio gradual declines. This is because with the increase of the superficial gas velocity, the upward drag force on the particles increases; the load of particles decreases; the particle spacing becomes larger; the closeness of the particles in the bed decreases; the porosity increases; and the bed expansion rate increases, altogether rendering it difficult for sticking loss to occur [11]. Furthermore, the metallization rate increases with the increase of the gas velocity.

When the linear velocity is 0.8 m/s, the minimum sticking ratio is 51.38%; when the linear velocity is 1.0 m/s, the sticking ratio increases to 78.71%. When the gas velocity is more than 1.0 m/s, some small particles of the reducing material are brought out from the fluidized bed. This is the reason why the metallization rate decreases when the gas velocity exceeds 1.0 m/s.

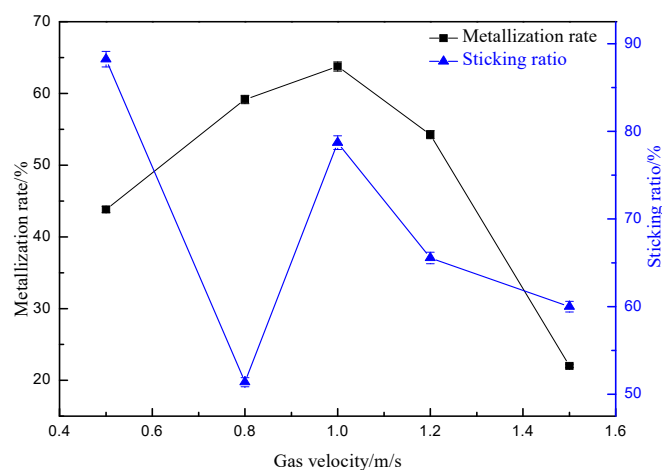


Figure 3. Trend of the metallization rate and sticking ratio with changing linear velocity when 0.18 mm–0.66 mm of OMC fine iron ore is reduced by pure carbon monoxide at 0.2 MPa, 1023 K after 50 min.

3.2. Influence of the Reduction Pressure

Under a reduction temperature of 1023 K and a linear velocity of 0.8 m/s, the reduction pressure of OMC fine iron ore with a particle size of 0.18 mm–0.66 mm was carried out. The trend of the metallization rate with changing pressure when the OMC fine iron ore is reduced by pure carbon monoxide for 50 min is shown in Figure 4.

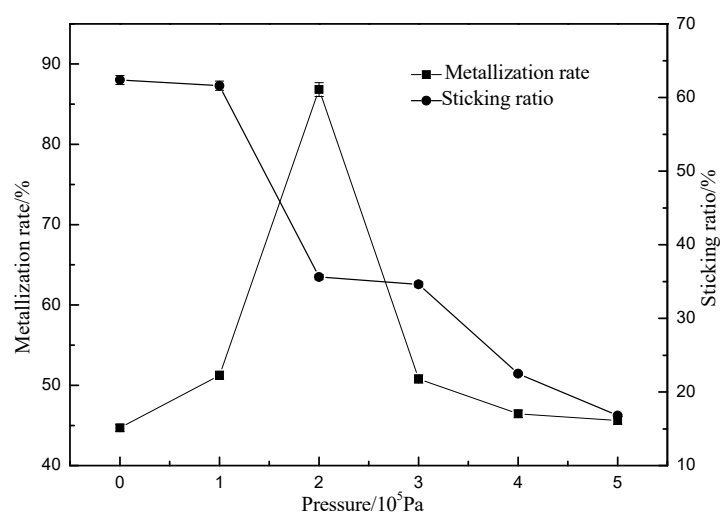


Figure 4. Trend of the metallization rate and sticking ratio with changing pressure when 0.18 mm–0.66 mm of OMC fine iron ore is reduced by pure carbon monoxide at 1023 K, 0.8 m/s after 50 min.

As shown in Figure 4, with the increase of the reduction pressure, the metallization rate increases first and then decreases. When the pressure is 0.2 MPa, the metallization rate reaches up to 86.82%. When the reduction pressures are atmospheric pressure, 0.1 MPa, 0.3 MPa, 0.4 MPa, and 0.5 MPa, the metallization rate fluctuates in the range of 44.70–51.25%. With the increasing of pressure, the sticking ratio exhibits a trend of oscillation with an overall decrease. When the reduction pressure is 0.5 MPa, the sticking ratio is the smallest but the metallization rate is relatively low; when the reduction pressure is 0.2 MPa, the sticking ratio is 35.62%, the sticking phenomenon is not found, and the metallization rate is the highest.

3.3. Influence of the Reduction Temperature

Under a linear velocity of 0.8 m/s and a reduction pressure of 0.2 MPa, the experimental study of OMC fine iron ore with a particle size of 0.18 mm–0.66 mm was carried out under different temperatures. Xu et al. [11] summarized the optimal operating parameters required to reduce fine iron ore to be in the range of 923 K to 1023 K temperatures, and therefore this temperature range was selected for the current study. The result is shown in Figure 5.

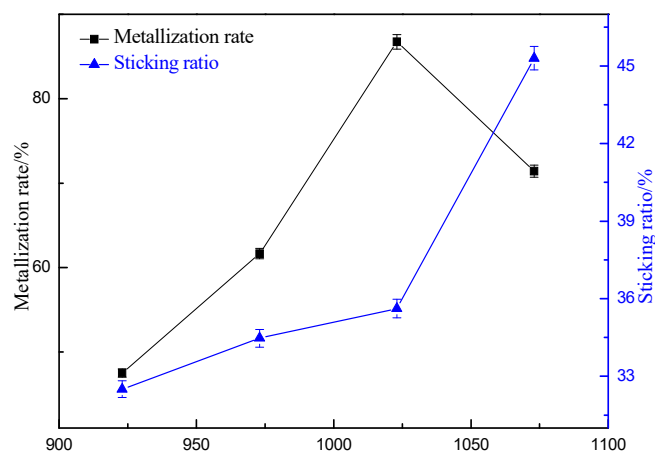


Figure 5. Trend of the metallization rate and sticking ratio with changing temperature when 0.18 mm–0.66 mm of OMC fine iron ore is reduced by pure carbon monoxide at 0.2 MPa, 0.8 m/s after 35 min.

As shown in Figure 5, there is a heating process when cold material is added to the experiment, causing the metallization rate to increase gradually. When the temperature reaches 1023 K, the metallization rate reaches the maximum value. As the temperature rises, the sticking ratio increases. When the temperature changes in the range of 923 K–1023 K, the sticking ratio increases slowly. When the temperature exceeds 1023 K, the sticking ratio increases significantly.

3.4. Influence of the Particle Size

With a linear velocity of 0.8 m/s, reduction pressure of 0.2 MPa, and reduction temperature of 1023 K, the reduction experiment of OMC fine iron ore with different particle sizes was carried out. The experimental results are shown in Figure 6.

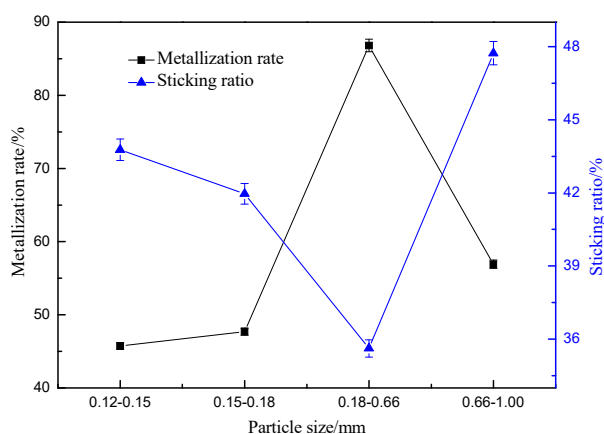


Figure 6. Trend of the metallization rate and sticking ratio with changing particle sizes when the OMC fine iron ore is reduced by pure carbon monoxide at 0.2 MPa, 1023 K, 0.8 m/s after 35 min.

As shown in Figure 6, the metallization rate increases first and then decreases with the reduction of the particle size, while the sticking ratio decreases first and then increases with the reduction of the particle size. When the particle size is in the range of 0.66 mm–1.00 mm, the metallization rate is 56.7% and the sticking ratio is 47.2%. When the particle size is in the range of 0.18 mm–0.66 mm, the metallization rate reaches the maximum, while the sticking ratio is at the minimum.

3.5. Influence of the Reduction Time

Under a reduction temperature of 1023 K, particle size of 0.18 mm–0.66 mm, and linear velocity of 0.8 m/s, pure carbon monoxide was used in the pressured test of the OMC fine iron ore. Under these conditions, the sticking phenomenon was not found after reductions of 50 min and 35 min. The sticking ratios at 35 min and 50 min were very close, but compared with the metallization rate of 35 min, the metallization rate of 50 min was increased significantly. The change trend of the metallization rate is shown in Figure 7.

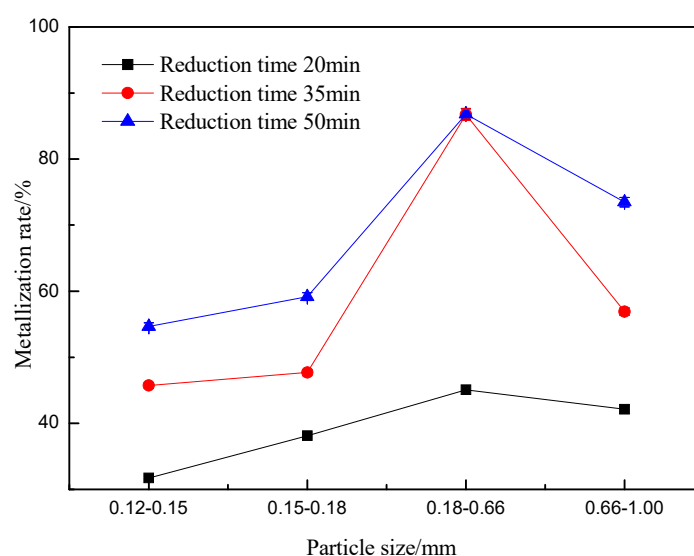


Figure 7. Trend of the metallization rate with changing particle sizes when the OMC fine iron ore is reduced by pure carbon monoxide at 0.2 MPa, 1023 K, 0.8 m/s after 20 min, 35 min, and 50 min.

As shown in Figure 7, the metallization rate increases first and then decreases with the increase of the particle size. When the particle size of fine iron ore is the same and the reduction time is less than 50 min, the longer the reduction time, the greater the metallization rate. When the particle size of fine iron ore is between 0.18 mm and 0.66 mm, the metallization rates of 35 min and 50 min are very close, and they are both greater than the metallization rate of 20 min.

3.6. Verification of the Optimum Operation Parameters for the Metallization Rate and Sticking Ratio

The relation between the metallization rate and sticking ratio for all experimental data of different samples (particle sizes) is shown in Figure 8. The best operating parameters for reducing fine iron ore by pure carbon monoxide are a linear velocity of 0.8 m/s, reduction pressure of 0.2 MPa, reduction temperature of 1023 K, and particle size in the range of 0.18 mm–0.66 mm. The influence of each factor is explained as follows.

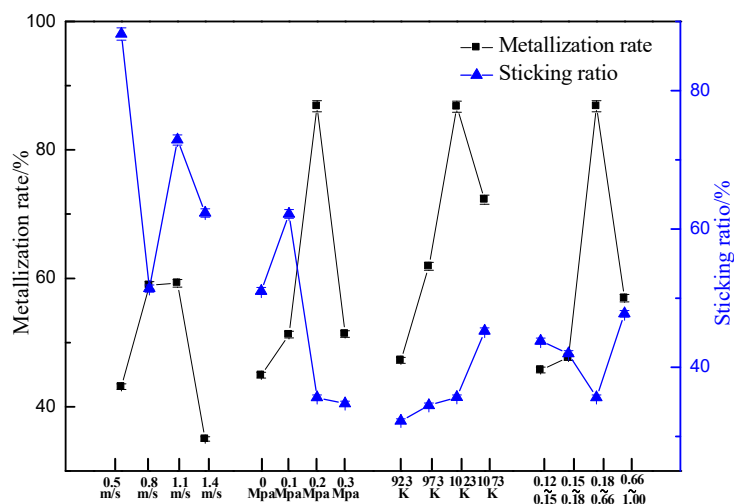


Figure 8. The relation between the metallization rate and sticking ratio of each factor.

3.6.1. Influence of the Pressure

(1) $0 \leq P < 0.2$ MPa

It is known that when the reduction pressure is less than 0.2 MPa, increases in the reduction pressure can effectively improve the metallization rate and reduce the sticking ratio, as shown in Figures 4 and 8. In the process of reducing fine iron ore by carbon monoxide, when the reduction pressure is increased, the two reactions in which Fe_2O_3 is reduced and carbon is precipitated are synchronous, as shown by the x-ray diffraction spectrogram in Figures 9 and 10. When the pressure is increased appropriately, the carbon precipitation reaction is accelerated and the metal iron precipitates on the surface of particles. However, the solute carbons from the carbon precipitation dissolve into metal iron to form Fe_3C . In the reduction process, Fe_2O_3 is restored into Fe by the carbon monoxide through reactions (3)–(5). In addition to the abovementioned iron oxide reduction reaction, the Boudouard reaction occurs:



Carbon atoms produced by reaction (6) and iron atoms will form Fe_3C , according to the reaction shown below:



This is because iron atoms catalyze the carbon reaction; moreover, as the carbon and iron atoms combine more closely, they soon form Fe_3C . Formula (6) is actually a synthesis of Formulas (3), (4), and (5). Therefore, the precipitated carbon will combine with the iron atoms to produce Fe_3C in the reduction reaction process.

A layer of Fe_3C forms between the graphite and metal iron, which further hinders the solid solution of graphite. Because of the barrier of metal iron layer, graphite on the surface cannot come into contact with oxygen atoms in the particles, which avoids the direct contact between irons and hinders the diffusion of atoms to form a solid bridge, eliminating the sticking force between the particles and causing the sticking loss to be completely inhibited. However, because the metallization rate of particles is low, the metal iron exists in the form of iron particles on the particle surface and does not form a metal layer. And with iron oxide distributed around, the precipitated carbon will react with iron oxide when the temperature rises, leading to a reduced amount of carbon and an increased amount of

metal iron. As the height of the peak in Figure 9 shows, compared with the reduction time of 35 min, the content of precipitated graphite and iron atoms both increase after 50 min of reduction. According to the peak height of Figure 10, compared with atmospheric pressure, the content of precipitated graphite increases under the pressure of 0.2 MPa, and the increasing amount of precipitated graphite can effectively restrain the occurrence of sticking and cause the metallization rate to increase, which is consistent with the results in Figure 4.

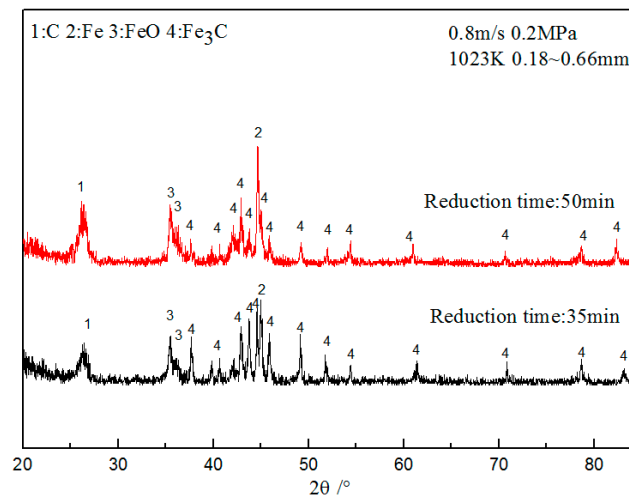


Figure 9. The X-ray diffraction spectrogram when 0.18 mm–0.66 mm of OMC fine iron ore is reduced by pure carbon monoxide at 0.2 MPa, 1023 K, 0.8 m/s after 35 min and 50 min.

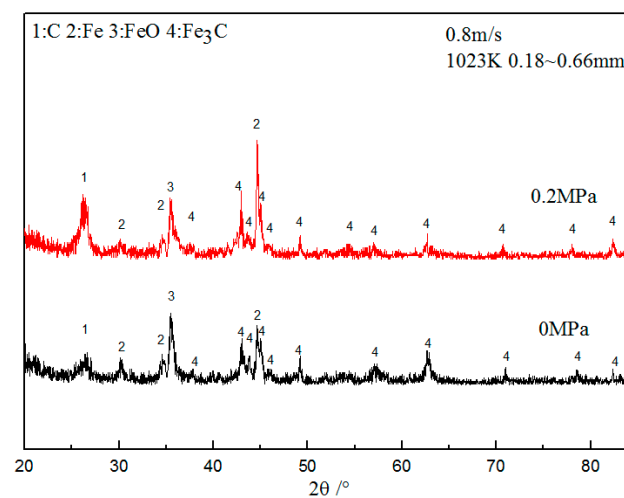


Figure 10. The x-ray diffraction spectrogram when 0.18 mm–0.66 mm of OMC fine iron ore is reduced for 50 min by pure carbon monoxide at 1023 K, 0.8 m/s, 0 MPa and 0.2 MPa.

(2) $0.2 \text{ MPa} \leq P$

It is known that the increase of the reduction pressure will lead to the reduction of the metallization rate when the reduction pressure is more than 0.2 MPa, as shown in Figures 4 and 8. The analysis of the microscopic morphology of the particles after reduction at 0.2 MPa is shown in Figure 11. In this figure, there is a layer of reduction material on the surface to wrap the particles. Because of the particle collision in the fluidization reduction process, there is a small amount of coating layer peeling off at the corner of the powder particles. Based on the results in Figure 11, a layer of metal iron formed on the surface of the particles, and the solute graphite on the iron layer reached saturation [21].

The increase of the pressure can promote the carbon precipitation of carbon monoxide, which can be seen from Formula (6); with the increase of the pressure, the rate of graphite precipitation is accelerated. Under 0.2 MPa, the metallization rate is the largest, and its value is 86.82%. When there is no iron oxide on the surface of particles, a layer of metal iron will form on the surface of the particle, and when the solute carbons on the iron layer reach saturation, a layer of Fe_3C will be formed, which further hinders the solid solution of graphite and causes the content of Fe_3C remain stable. The outermost part is the graphite layer, the middle part is the Fe_3C layer, and the inside part is the metal iron layer. This shows that under the condition of increased pressure, the graphite precipitation of the carbon monoxide is promoted to make a layer of graphite attached to the surface of particles, and this graphite is the main factor inhibiting sticking loss, which is consistent with the reported opinion [21–24]: graphite and the carbon in Fe_3C can slow down the sticking loss of fine iron ore.

Based on the above analyses, the appropriate pressure is 0.2 MPa.

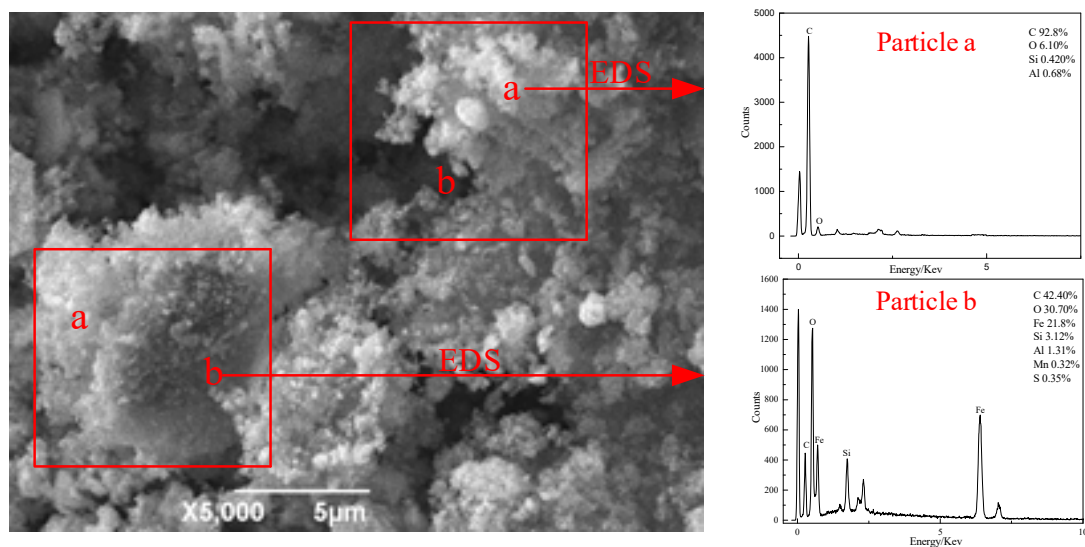


Figure 11. SEM diagram of the surface morphology of OMC fine iron ore particles after reduction by pure carbon monoxide at 1023 K, 0.8 m/s, 0.2 MPa.

3.6.2. Influence of the Gas Linear Velocity, Particle Size when the Pressure is 0.2 MPa

Xu Qiyuan and Guo Lei [11,25] found that the drag force of gas on a single particle can be expressed by the following formula:

$$F_d = 25 \frac{\pi(1-\varepsilon)}{\varepsilon^3} \times \mu_g u d_p + 0.29 \frac{\rho_g u^2 d_p^2}{\varepsilon^3} \quad (7)$$

where F_d is the drag force of gas on the particle, N; ε is the fluidized bed void fraction with no dimension; μ_g is the gas viscosity, kg/(m·s); u is apparent gas velocity, m/s; d_p is the particle diameter, m; and ρ_g is the gas density, kg/m³.

It can be seen from Formula (7) that the larger particle size, the greater the drag force of gas on particles, and the less likely sticking is to occur. Therefore, properly increasing the particle size can significantly improve the metallization rate, but the particle size limit is that the starting fluidizing velocity of large particle must be less than the superficial setting. Also, the increase of particle momentum is conducive to reducing the particle sticking tendency [19], but the effect and mechanism of particle size on the sticking loss are also related to the linear velocity of metallization.

(1) Gas Linear Velocity ≤ 0.8 m/s

The larger the linear velocity, the greater the drag force, and the greater the kinetic energy needed to overcome sticking, resulting in smaller sticking trends. In a certain range, the sticking presents a decreasing trend with the increase of the gas velocity.

When the range of particle size is between 0.66 and 1.0 mm, the fluidization effect is not obvious. The larger the particle size, the smaller the gas-solid contact area, and the more unfavorable the gas-solid reaction. If the reduction reaction stays on the gas-solid surface, the iron whisker will lead to sticking loss [11]. Moreover, with the occurrence of particle clustering, and the particle size becoming larger, the linear velocity will not be sufficient to achieve the metallization of iron ore, and it will cause complete sticking.

The experiment showed that as the range of particle size decreases from 0.66–1.0 mm to 0.18–0.66 mm, the metallization rate increases and the sticking ratio is reduced. As the range of particle size decreases from 0.18–0.66 mm to 0.12–0.18 mm, the metallization rate also decreases and the sticking ratio increases.

When the particle size is in the ranges of 0.15 mm–0.18 mm and 0.12 mm–0.15 mm, the surface area of particles is large; the gas-solid reaction proceeds rapidly, and the reduction of fine iron ore exhibits early iron precipitation. When the linear velocity is under the same condition, the smaller the fine iron ore particles are, the easier they are to bond. The reaction is mainly characterized by carbon precipitation along with the decrease of the metallization rate.

(2) Gas Linear Velocity >0.8 m/s

When the sticking force is over the drag force, the iron whiskers will reunite and this will lead to sticking loss. When the linear velocity exceeds 1.0 m/s, the particles are more prone to slipping, and some small particles of the reducing material are brought out from the fluidized bed. When the particle spacing in the bed is small, the expansion rate of the bed layer decreases gradually with the increase of particles, increasing the sticking ratio and leading to a decrease in the metallization rate.

When the linear velocity is over 1.5 m/s, the gas drag force on the particles is over the sum of the particle cohesion and the force of gravity, and this will lead to fine iron ore particles being brought out from the fluidized bed.

Based on the above analysis, the appropriate linear velocity and particle size are respectively 0.8 m/s and 0.18–0.66 mm.

3.6.3. Influence of the Reduction Time and Reduction Temperature when the Pressure is 0.2 MPa

As can be seen from Figure 9, in terms of peak height ratios relative to FeO peaks, the reduction of 50 min is higher than the reduction of 35 min. Compared with reduction time of 35 min, the content of precipitated graphite and iron atoms both increase after 50 min of reduction. The sticking phenomenon was not found in the observation window when the reduction time was 35 min or 50 min, but when the reduction time was extended to 55 min, 60 min, and 65 min, the sticking phenomenon appeared and gradually increased, and sticking ratio also gradually increased.

With the increase of the temperature, the iron whisker energy generated from the reduction on the surface of particles is higher. Also, with the force between the iron whiskers increasing, high energy iron whiskers can agglomerate more easily, causing sticking loss, a reduction of the metallization rate, and an increase in the sticking ratio. At the same time, when the reduction temperature increases, the diffusion rate of the iron atoms and the sticking rate will accelerate, leading to the occurrence of sticking loss.

At the beginning of sintering, the iron atoms diffuse on the surface. The diffusion rate of the iron atoms can be expressed by the following Formula [26]:

$$D_S = D_{0,S} \exp\left(-\frac{E_S}{RT}\right) \quad (8)$$

where, D_s is surface iron atoms' diffusion coefficient, m^2/s ; $D_{0,s}$ is surface iron atoms' self-diffusion coefficient, m^2/s , $D_{0,s} = 5.2 m^2/s$; and E_s is surface iron atoms' diffusion activation energy, J/mol , $E_s = 2.21 \times 10^5 J/mol$ [27].

The relationship between D_s and temperature can be estimated through the formula above, and as shown in Figure 12. As can be seen from Figure 12, when the temperature is below 1023 K, the surface iron atoms' diffusion coefficient is stable. However, when the temperature exceeds 1023 K, the metal surface particles' diffusion coefficient increases with the increase of the temperature [28–30]. Thus, the higher the temperature, the greater the sticking force between particles. This relationship exhibited an increasing trend, which is consistent with the results in Figure 5. A heating process was conducted after the addition of the cold material, so that the metallization rate could increase with the reduction reaction. When the temperature reaches a certain degree, the metallization rate reaches the maximum value. At low temperatures, the sticking ratio is maintained at a low level with excellent efficiency. With the increase of the temperature, the sticking ratio increases gradually and the sticking progressively deteriorates. It is known that with the rise in temperature, the sticking ratio increases and the metallization rate increases first and then decreases, as shown in Figures 5 and 8. With the increase of the temperature, the energy of the surface of the particles produced by the reduction also increases, which in turn increases the physical adsorption, making the energy of the iron whisker more prone to amalgamation, thus leading to sticking adhesion.

Based on the above analysis, the appropriate reduction time and reduction temperature are respectively 50 min and 1023 K.

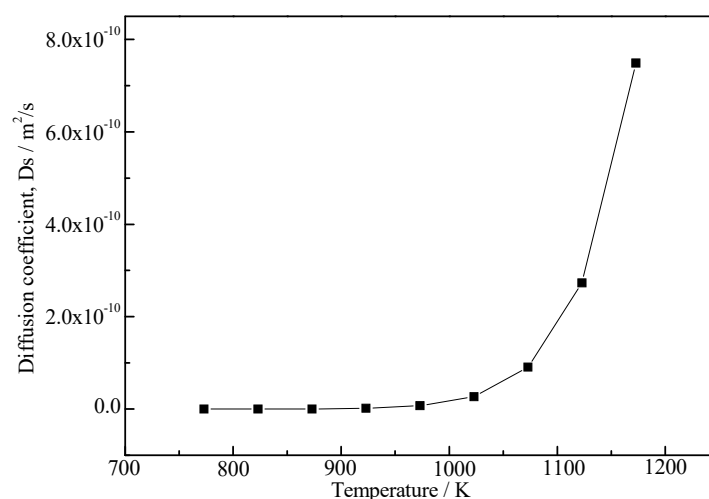


Figure 12. The relationship between the diffusion coefficient and temperature.

4. Conclusions

- (1) The best operating parameters for reducing fine iron ore by pure carbon monoxide are as follows: linear velocity of 0.8 m/s, reduction pressure of 0.2 MPa, reduction temperature of 1023 K, reduction time of 50 min, and particle size in the range of 0.18 mm–0.66 mm.
- (2) The proper pressure can promote the carbon precipitation of carbon monoxide and helps to increase the metallization rate. Upon increasing of reduction pressure from 0 MPa to 0.5 MPa, the metallization rate increases first and then decreases. Under 0.2 MPa, the metallization rate is the largest, and its value is 86.82%.
- (3) The graphite produced by carbon monoxide precipitation prevents the diffusion of iron atoms and avoids direct contact between iron atoms, which is the main factor inhibiting the sticking of fine iron ores.

Author Contributions: Q.X., J.W. and H.W. designed and performed the experiments; Q.X., J.W. and H.W. analyzed and discussed the data; Q.X. provided guidance for this research; Q.X. wrote the paper.

Funding: This research was founded by the National Natural Science Foundation of China, grant number 51704003, and the financial support of Anhui province natural science research project, grant number KJ2017A043.

Conflicts of Interest: The authors declare no conflict of interest.

References

1. Yang, T.J.; Zhang, J.L.; Zuo, H.B. Energy-Saving and Emission-Reducing of Blast Furnace Ironmaking Production in China. *J. Iron Steel Res. Int.* **2009**, *16*, 591–596.
2. Zheng, Z.; Lin, L.C.; Chen, Z.W.; Lim, J.; Grace, J. A dual-scale lattice gas automata model for gas–solid two-phase flow in bubbling fluidized beds. *Comput. Math. Appl.* **2011**, *61*, 3593–3605. [[CrossRef](#)]
3. Wang, Z.Y.; Zhang, J.L.; Jiao, K.X.; Liu, Z.J. Effects of Pre-Reduction Degree of Ironsand on Slag Properties in Melting Separation Process. *Steel Res. Int.* **2018**, *89*, 1700363. [[CrossRef](#)]
4. Liu, D.H.; Wang, X.Z.; Zhang, J.L.; Liu, Z.J.; Jiao, K.X.; Liu, X.L.; Wang, R.R. Study on the controlling steps and reduction kinetics of iron oxide briquettes with CO-H₂ mixtures. *Metall. Res. Technol.* **2017**, *114*, 611. [[CrossRef](#)]
5. Zhang, S.R.; Zhang, S.X. Finex process at posco steel corporation in Korea. *Iron Steel* **2009**, *44*, 1–5.
6. Tang, H.Q.; Yun, Z.W.; Fu, X.F.; Du, S. Modeling and experimental study of ore-carbon briquette reduction under CO–CO₂ atmosphere. *Metals* **2018**, *8*, 205. [[CrossRef](#)]
7. Bizhanov, A.; Malysheva, T. Metallization of extruded briquettes (BREX) in midrex process. *Metals* **2017**, *7*, 259. [[CrossRef](#)]
8. Yang, M.; Xiao, W.D.; Zhang, P. Processing mineralogy study on lead and zinc oxide ore in Sichuan. *Metals* **2016**, *6*, 93. [[CrossRef](#)]
9. Tang, J.; Chu, M.S.; Ying, Z.W.; Li, F.; Feng, C.; Liu, Z.G. Non-Isothermal gas-based direct reduction behavior of high chromium vanadium-titanium magnetite pellets and the melting separation of metallized pellets. *Metals* **2017**, *7*, 153. [[CrossRef](#)]
10. Shi, Y.J.; Liu, S.J.; Yao, J.Z.; Li, G.L. Carbon adhesion and reduction of iron ore powder in a fluidized bed. *Iron Steel* **1993**, *28*, 1–7.
11. Xu, Q.Y.; Wang, H.C.; Fu, Y.K.; Wang, J.J. Parameters optimization, sticking mechanism and kinetics analysis of fine iron ore in fluidized-reduction process. *ISIJ Int.* **2016**, *56*, 1929–1937. [[CrossRef](#)]
12. Shao, J.H.; Guo, Z.C.; Tang, H.Q. Influence of reducing atmosphere on the sticking during reduction of iron ore fines in a fluidized bed. *J. Univ. Sci. Technol. Beijing* **2013**, *35*, 273–281.
13. Bohn, C.D.; Cleeton, J.P.; Müller, C.R.; Davidson, J.F.; Hayhurst, A.N.; Scott, S.A.; Dennis, J.S. The Kinetics of the reduction of iron oxide by carbon monoxide mixed with carbon dioxide. *AIChE J.* **2010**, *56*, 1016–1029. [[CrossRef](#)]
14. Gao, K.; Wu, J.H.; Wang, Y. The modeling research of the ash-agglomerated fluidized bed gasifier. *J. Fuel Chem. Technol.* **2006**, *34*, 670–674.
15. Huang, J.J.; Fang, Y.T.; Wang, Y. Development and progress of modern coal gasification technology. *AIChE J.* **2002**, *30*, 385–391.
16. Sidorenko, I.; Rhodes, M.J. Influence of pressure on fluidization properties. *Powder Technol.* **2004**, *141*, 137–154. [[CrossRef](#)]
17. Kawabata, J.I.; Yumiyama, M.; Tazaki, Y.; Honma, S. Characteristics of gas-fluidized bed under pressure. *J. Chem. Eng. Jpn.* **1981**, *14*, 85–89. [[CrossRef](#)]
18. Krebs, V.; Elalaoui, M.; Mareche, J.F.; Furdin, G.; Bertau, R. Carbonization of coal-tar pitch under controlled atmosphere-Part I: Effect of temperature and pressure on the structural evolution of the formed green coke. *Carbon* **1995**, *33*, 645–651. [[CrossRef](#)]
19. Lee, Y.J.; Joo, H.J. Investigation on ablation behavior of CFRC composites prepared at different pressure. *Compos. A Appl. Sci. Manuf.* **2004**, *35*, 1285–1290. [[CrossRef](#)]
20. Gong, Q.M.; Huang, Q.Z.; Huang, B.Y.; Wu, F.Q.; Chen, T.F.; Zhang, F.Q. Effect of carbonization pressure on morphology of pitch derived carbon and densification efficiency of C/C composites used for aircraft brakes. *New Carbon Mater.* **2002**, *17*, 23–28.

21. Zhang, B.; Wang, Z.; Gong, X.Z.; Guo, Z.C. Characterization of precipitated carbon by XPS and its prevention mechanism of sticking during reduction of Fe₂O₃ particles in the fluidized bed. *ISIJ Int.* **2013**, *53*, 411–418. [[CrossRef](#)]
22. Klug, J.H. Process to Reduce Sticking During Surface Treatment of Graphite Articles. U.S. Patent 6,702,970, 9 March 2004.
23. Shao, J.; Guo, Z.; Tang, H. Effect of Coating MgO on Sticking Behavior during Reduction of Iron Ore Concentrate Fines in Fluidized Bed. *Steel Res. Int.* **2013**, *84*, 111–118. [[CrossRef](#)]
24. Miyagawa, K.; Kamijo, T.; Deguchi, M. Sticking and Its Prevention in Fluidized Bed Reduction of Iron Ores (In-bath Smelting and Fluidized Bed Reduction). *Tetsu Hagane* **2009**, *78*, 1258–1265. [[CrossRef](#)]
25. Guo, L.; Gao, H.; Yu, J.T.; Zhang, Z.L.; Guo, Z.C. Influence of hydrogen concentration on Fe₂O₃ particle reduction in fluidized beds under constant drag force. *Int. J. Miner. Metall. Mater.* **2015**, *22*, 12–20. [[CrossRef](#)]
26. Langston, B.G.; Stephens, F.M. Self-agglomerating fluidized bed reduction. *JOM* **1960**, *12*, 312–316. [[CrossRef](#)]
27. Matsumu, G. Sintering of Iron Wires. *Acta Metall.* **1971**, *19*, 851–855. [[CrossRef](#)]
28. Wang, Q.; Zou, X.; Matsuura, H.; Wang, C. Evolution of Inclusions During the 1473 K (1200 °C) Heating Process of EH36 Shipbuilding Steel. *Metall. Mater. Trans. B* **2018**, *49*, 18–22. [[CrossRef](#)]
29. Zou, X.; Zhao, D.; Sun, J.; Wang, C.; Matsuura, H. An Integrated Study on the Evolution of Inclusions in EH36 Shipbuilding Steel with Mg Addition: From Casting to Welding. *Mater. Trans. B* **2017**, *49*, 481–489. [[CrossRef](#)]
30. Xue, Q.; Ma, Y.J.; Lei, J.F.; Yang, R.; Wang, C. Evolution of microstructure and phase composition of Ti-3Al-5Mo-4.5V alloy with varied β phase stability. *J. Mater. Sci. Technol.* **2018**, in press. [[CrossRef](#)]



© 2018 by the authors. Licensee MDPI, Basel, Switzerland. This article is an open access article distributed under the terms and conditions of the Creative Commons Attribution (CC BY) license (<http://creativecommons.org/licenses/by/4.0/>).